Biophysical Chemistry, 36 (1990) 187–199
Elsevier

BIOCHE 01444

Interpreting the visible absorption bands of 1,4-(dihydroxy)-9,10-anthraquinone and its metal chelates

Todd S. Koch and Richard P. Rava

Chemistry Department, State University of New York, University Center at Binghamton, Binghamton, NY 13901, U.S.A.

Received 5 January 1990
Accepted 5 January 1990

Absorption spectroscopy; Electronic spectroscopy; Anthracycline

The visible absorption spectra of 1,4-(dihydroxy)-9,10-anthraquinone and of Co(II), Ni(II), Cu(II) and Zn(II) chelates have been studied in different organic solvents. This system provides a model for the anthracycline antibiotics and their metal chelates. The band structure of the spectrum has been determined using the second and fourth derivatives of the spectrum. The visible absorption band of the parent molecule can be assigned to a single electronic state with a reduced dipole moment in the excited state; structure in this band is ascribed to two overlapping vibrational progressions. In contrast, the dianion (hydroxy protons removed) shows a single electronic state with an increased dipole moment in the excited state; structure in this band can be assigned to a single vibrational progression. All of the metal chelates show spectra which are similar in appearance to that of the dianion although the identity of the metal determines the bathochromic shift of the absorption band. Titration of 1,4-dihydroxyanthraquinone with $Cu(ClO_4)_2 \cdot 6H_2O$ demonstrates that three chelates with metal-to-ligand ratios of 1:2, 1:1 and 2:1 can form depending on the identity of the metal, ratio of metal to ligand, and donor character of the solvent.

1. Introduction

Hydroxyquinones are compounds of significant chemical and biochemical interest. These molecules have found important applications as a prominent family of pharmaceutically active and biologically relevant chromophores, as an analytical tool for the determination of metals, and in many aspects of electrochemistry [1]. Their chemistry is often monitored via visible absorption spectroscopy and the results used to determine chemical and biochemical mechanisms of activity. Yet, a fundamental understanding of the electronic properties of these systems has remained elusive.

The chelating properties of these chromophores play an important role in their chemistry and biochemistry. A number of papers concerning the characterization of metal chelates of hydroxybenzoquinones, hydroxynaphthoquinones and hydroxyanthraquinones have been published but an examination of the electronic properties has not been undertaken [2–16]. The large change in the absorption spectrum of solutions of hydroxyquinones upon addition of metal salts appears to indicate altered electronic properties. An example is the absorption spectrum obtained from the addition of a copper(II) salt to an ethanolic solution of 1,4-(dihydroxy)-9,10-anthraquinone (1,4-$(OH)_2$-AQ, structure shown in fig. 1) as shown in fig. 2. The absorption spectrum of the copper chelated species has not been assigned.

1,4-$(OH)_2$AQ is the smallest molecule showing the chromophore characteristic of the anthracy-

Correspondence (present) address: R.P. Rava, George R. Harrison Spectroscopy Laboratory, Massachusetts Institute of Technology, Cambridge, MA 02139, U.S.A.

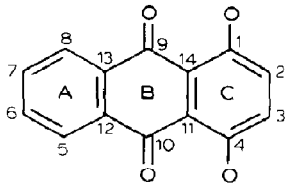

Fig. 1. Structure of 1,4-dihydroxyanthraquinone. Atom numbering is utilized for π-electron coefficients in tables 2 and 4.

cline antibiotics, doxorubicin and daunorubicin [17,18]. Although intercalation into nuclear DNA has been considered to be the classical mechanism for the action of these drugs, recent studies have indicated that intercalation may not be a sufficient condition for the drugs to show antitumor activity [19]. It has been suggested that the metal chelates of these drugs play a major role in their activity by altering the redox properties of the drug [20]. Several reports of the visible absorption and vibrational spectroscopy of the metal chelates of doxorubicin and daunorubicin have been published [21–30], but do not provide quantitative information on the electronic properties of these systems.

A major difficulty in understanding the electronic properties of the hydroxyanthraquinones is the broad visible absorption spectrum observed in solution. A small amount of fine structure is apparent, but it is difficult to assign the features to particular excited states or vibrational bands. Careful choice of solvent or lowering the temperature of the system does permit the vibronic structure to be better scrutinized allowing assignment of the individual bands [31–38], but nonetheless the spectrum remains broad enough to obscure much of the potential information.

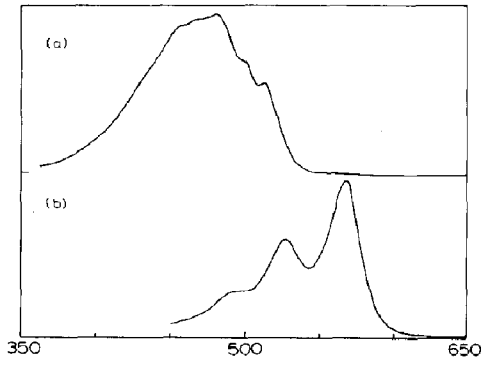

Fig. 2. Visible absorption spectrum of (a) 1,4-dihydroxyanthraquinone in ethanol (1 mM) and (b) 1,4-dihydroxyanthraquinone (1 mM) with $Cu(ClO_4)_2 \cdot 6H_2O$ (5 mM) in ethanol.

Our approach is to examine the visible absorption spectra in different solvents at room temperature using derivative techniques. These methods have been discussed in the literature for over 30 years [39–44] and much of the theoretical groundwork was determined in the early seventies; however, the techniques seem to have been embraced mainly as analytical procedures rather than to aid in the interpretation of solution electronic spectra. In previous work we have demonstrated the utility of these methods for understanding the absorption spectroscopy of colchicine in solution and bound to the protein tubulin [45]. In this paper, we will use the second and fourth derivatives of the absorption spectra to study the equilibrium formation of the different metal chelates, and assign their electronic properties.

In section 2 we will discuss the experimental and theoretical details. The visible absorption spectra of 1,4-$(OH)_2$AQ and the deprotonated dianion (1,4-O_2AQ^{2-}) are analyzed in sections 3.1 and 3.2, respectively, making use of semi-empirical MNDO calculations [46] to aid the electronic assignments. The visible absorption spectra of the metal chelates of Co(II), Ni(II), Cu(II) and Zn(II) are discussed in section 3.3.

2. Experimental

1,4-$(OH)_2$AQ and metal salts were obtained from Aldrich and used as supplied. Spectra grade solvents were dried over molecular sieves prior to use, and a 1 mM solution of 1,4-$(OH)_2$AQ was prepared in the organic solvent of interest. No evidence of dimer formation, as judged by changes in the absorption spectra of these systems [47], was observed in the organic solvents used in this study. Metal salts were also dissolved in the same solution to a stoichiometric ratio of one metal ion

to one 1,4-$(OH)_2$AQ or two metal ions to one 1,4-$(OH)_2$AQ. Additionally, a stoichiometric amount of triethylamine equivalent to the amount of metal was added to the solution to facilitate complex formation. A precipitate was formed immediately if the amount of triethylamine added was greater than the amount of metal. Previous work suggests that a polymer is formed with a 1 : 1 ratio of metal to ligand under these conditions [26]. A polymer also appeared to be formed in high-pH solutions of pure 1,4-$(OH)_2$AQ.

Several different salts of Zn(II), Cu(II), Ni(II) and Co(II) were tested. Metal complexes of 1,4-$(OH)_2$AQ were readily formed with perchlorate and nitrate salts; however, acetate and sulfate salts did not give good yields of the chelates. Halide salts led to better yields than acetate or sulfate but poorer than perchlorate or nitrate. The observed spectral features are unaffected by the choice of anion, suggesting that the differences observed for the formation of complexes are due primarily to a lack of complete dissociation of the metal salts in the nonaqueous solvents. The results discussed employed perchlorate salts; in the case of zinc the perchlorate salt was unavailable, and a nitrate salt was utilized. All of the spectra are reported for hexahydrate forms of the salts, although we did not observe any alteration of the electronic properties in the visible absorption spectrum with different hydrated forms.

Similar species of metal chelates could be obtained if large excesses of the metal salt were added in lieu of stoichiometric amounts of triethylamine. A titration of 1,4-$(OH)_2$AQ with $Cu(ClO_4)_2 \cdot 6H_2O$ in ethanol was carried out by adding microliter quantities of the 0.1 M Cu(II) solution to a 1 mM solution of 1,4-$(OH)_2$AQ. Intensities (corrected for dilution) were measured at wavelengths established to correspond to the bands of different species in solution, and plotted vs equivalents of Cu(II).

Visible absorption spectra were recorded on a Hewlett-Packard model 8451A diode array spectrometer from 300 to 700 nm using a 1 mm path length cell. Digitization of the spectra at 2-nm intervals was carried out by the spectrometer and input into an IBM PC AT for numerical differentiation. Similar to our previous work [45], derivatives were carried out using the techniques described by Butler and Hopkins [42,43]. These authors showed both experimentally and theoretically that up to 4-fold enhancement in the signal-to-noise ratio of the fourth derivative spectra could be obtained by careful consideration of the derivative intervals. In the derivatives reported in this work, successive derivatives are taken from lower order derivatives with the first derivative numerically calculated for absorption intensity differences every 10 nm, the second every 6 nm, the third every 4 nm, and the fourth every 2 nm, leading to the correct intervals required to achieve the best signal-to-noise ratio. No data smoothing was found to be necessary when using this procedure.

3. Results and discussion

3.1. 1,4-Dihydroxyanthraquinone

3.1.1. Visible absorption spectrum

The visible absorption spectrum of 1,4-$(OH)_2$AQ has been the center of several studies [31,37,38]. Interest in the past several years has focused on the photochemical hole burning in an alcoholic matrix proposed to be due to rearrangement of intramolecular hydrogen bonding [48,49]. Measurements of the Stark effect at low temperature and study of the visible absorption spectrum in solvents of varying polar characteristics demonstrate that the transition in the visible region is to a state of decreased dipole moment [31], and thus this transition has been ascribed to a charge transfer excitation from the hydroxyl group to the carbonyl moiety.

Our intention in studying the visible absorption spectrum of 1,4-$(OH)_2$AQ in several different solvents is two-fold. The first objective is to demonstrate the power of the derivative methods discussed above for understanding the overlapping bands in the visible absorption spectrum of this compound. The derivative techniques allow us to assign individual vibrational transitions in the room temperature solution spectra, and study the behavior of the individual vibrations as a function of solvent properties. The second purpose is to

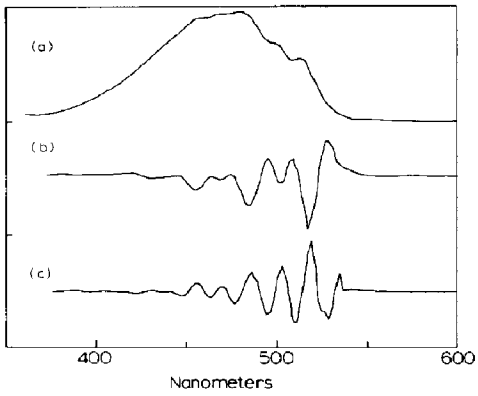

Fig. 3. Visible absorption spectrum of (a) 1,4-dihydroxyanthraquinone in ethanol (1 mM); (b) second derivative of the spectrum in (a); and (c) fourth derivative of the spectrum in (a). Both (b) and (c) have been scaled so that the derivatives could be compared with the original spectrum.

test the predictions of MNDO semi-empirical calculations on the transitions expected for these systems. The MNDO calculations of the ground-state molecular orbitals can be used to predict the alteration in the dipole moment for the visible transition. Also, the expected activity of the particular vibrational modes can be deduced from the bond order changes which take place upon electronic excitation.

The absorption spectrum, and second and fourth derivatives of the absorption spectrum of 1,4-$(OH)_2$AQ in ethanol are shown in fig. 3. The observed bands in ethanol and their assignments are listed in table 1. All of the bands observed in the fourth derivative spectrum can be correlated with vibrational bands assigned in previous work; however, the derivative methods allow the prominent progressions to be characterized to higher vibrational levels. The bands shift to higher energy in solvents of greater polarity which also concurs with previous work [31], and suggests that all the bands belong to a single excited state. In hydrogen-bonding solvents, such as ethanol, the bands are shifted to an energy higher than would be expected based simply on the polarity of the solvent. The molecular orbitals calculated using MNDO methods account for this dependence on polarity (vide infra).

Table 1

Wavelengths of the observed fourth derivative bands of 1,4-$(OH)_2$AQ in ethanol and their assignments

Wavelength (nm)	Assignment	Frequency above origin (cm^{-1})	
		This work	Ref. 37
515	0-0	0	0
501	ν_1	550	500
487	$2\nu_1$ or ν_2	1110	1007
481	ν_3	1370	1324
468	$\nu_1+\nu_3$	1950	1851
455	$2\nu_1+\nu_3$	2560	2574
442	$\nu_1+2\nu_3$	3270	
429	$2\nu_1+2\nu_3$	3890	

Two vibrational modes possess most of the vibrational activity in this excited state. The first mode, ν_1, has a frequency of approx. 550 cm^{-1}, and the second, ν_3, a frequency of approx. 1370 cm^{-1}. Previous assignments for these vibrations suggest that ν_1 is either an in-plane C=O wagging mode, δ(C=O), or a skeletal deformation mode; ν_3 is believed to be due to an O–H wagging vibration, δ(O–H) [37]. The disappearance of the ν_1 frequency in the spectra of the dianion and metal chelates indicates that the most likely assignment for this vibration is δ(C=O). Bond order changes determined from the MNDO calculations discussed below indicate that the ν_3 vibration is mainly made up of symmetric C–O stretching internal coordinates.

3.1.2. MNDO calculations

The π-electron coefficients for the highest occupied molecular orbital (HOMO) and the lowest unoccupied molecular orbital (LUMO) as determined from MNDO calculations of the ground state are given in table 2. The X-ray crystal structure geometry was used [50]. These calculations are being employed to gain a qualitative understanding of the character of the transition assigned to the visible absorption band rather than to predict quantitative information. If the latter was our intention, we would be required to carry out a full configuration interaction analysis of the system. This simple orbital method is convenient in yielding an intuitively useful picture of the first excited state of this molecule.

According to the MNDO results, the excitation of an electron from the HOMO to the LUMO

Table 2

π-electron coefficients for the HOMO and LUMO of 1,4-$(OH)_2$AQ as determined from MNDO calculations

Atom	HOMO	LUMO
O1	0.346	0.072
O9	0.132	−0.303
O4	−0.341	−0.071
O10	−0.135	0.299
C1	−0.413	−0.161
C2	−0.234	−0.265
C3	0.222	0.263
C4	0.418	0.163
C11	0.370	−0.259
C10	0.035	−0.291
C12	−0.007	−0.296
C5	−0.041	0.092
C6	−0.027	0.244
C7	0.021	−0.233
C8	0.041	−0.106
C13	0.013	0.299
C9	−0.038	0.301
C14	−0.366	0.252

moves electron density from the hydroxyl region of the molecule over to the carbonyl and the anthracene ring system. This correlates well with the recent suggestion of Johnson et al. [31] that this transition is primarily a charge-transfer-like excitation, with the electron going from the hydroxyl to the carbonyl moiety. The excitation results in a molecule with reduced dipole moment in the excited state, in agreement with experimental observations of a shift to higher energy for this transition in solvents of increased polarity.

The internal coordinates undergoing the largest displacement in the excited state will show the largest activity for an electronically allowed transition. In order to determine the internal coordinates undergoing the largest displacement, the change in the π-bond order upon HOMO to LUMO excitation was calculated. The result, shown in fig. 4, indicates that the primary displaced coordinate contains symmetric C–O stretching character coupled to C-C stretching character in the C ring. A mode with these internal coordinates is calculated at 1260 cm^{-1} in the ground state [51,52], correlating well with the observed excited-state frequency of ν_3. Therefore, a revised assignment for ν_3 in the excited state to a

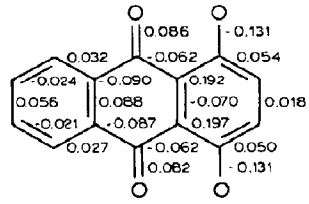

Fig. 4. The π bond order changes for the HOMO to LUMO transition in 1,4-dihydroxyanthraquinone as determined from MNDO calculations.

mode of this character is suggested. Discussion of the assignment of ν_1 will be included in our analysis of the spectrum of 1,4-O_2AQ^{2-}.

3.2. Dianion of 1,4-dihydroxyanthraquinone

3.2.1. Absorption spectroscopy

Binding a metal ion to the anthracycline antibiotics or 1,4-$(OH)_2$AQ results in a decrease in the pH of the solution. ^{1}H-NMR spectra of Yb(III) complexes [53] suggest specific binding of the metal ion between the carbonyl and hydroxyl oxygens. Thus, the metal ion actually binds to an anionic form of 1,4-$(OH)_2$AQ. In this section the visible absorption spectrum of the dianion of 1,4-$(OH)_2$AQ (1,4-O_2AQ^{2-}) is discussed. *

The absorption spectrum, and second and fourth derivatives of the absorption spectrum of 1,4-O_2AQ^{2-} in DMSO are shown in fig. 5. DMSO is chosen as a representative solvent because polymer formation does not appear to be a problem at high pH in this solvent. In contrast with the overlapping vibrational progressions found for 1,4-$(OH)_2$AQ, the dianion spectrum shows only three distinct bands following a simple Franck-Condon intensity pattern. A listing of the observed bands in DMSO and their assignments is given in table 3. There is some indication in the fourth derivative of splitting of these bands, possi-

* Attempts to obtain the spectrum of the monoanion species failed due to the difficulty associated with maintaining the small range of pH within which this species is stable. There is one reported spectrum of an anionic form of 1,4-$(OH)_2$AQ in the literature [48] which has been assigned to a monoanionic species; however, the energy of the bands matches those found for 1,4-O_2AQ^{2-} in this work.

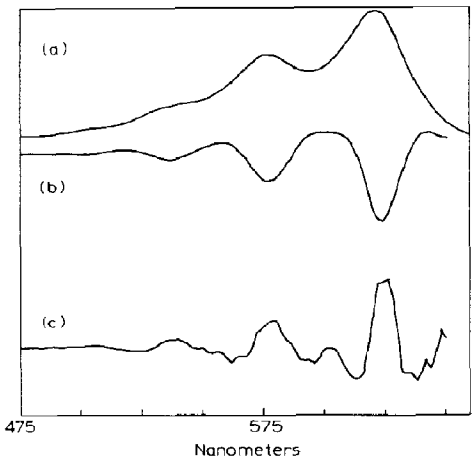

Fig. 5. (a) Absorption spectrum of the dianion of 1,4-dihydroxyanthraquinone formed by deprotonation; (b) second derivative of the spectrum in (a); and (c) fourth derivative of the spectrum in (a).

bly due to a low-frequency vibrational mode, but it is difficult to discern the additional peaks. All of the bands shift to lower energy in solvents of higher polarity, contrasting with the results for 1,4-$(OH)_2$AQ, and indicating that the excited state of 1,4-O_2AQ^{2-} has a higher dipole moment than the ground state. In hydrogen bonding solvents, however, the spectra are shifted to higher energy.

The observed vibrational pattern suggests primary activity is in a single active mode. In particular, activity of the low-frequency ν_1 vibration of 1,4-$(OH)_2$AQ is diminished in the spectrum of 1,4-O_2AQ^{2-}. This would be expected since the δ(C=O) frequency should be greatly altered in 1,4-O_2AQ^{2-}. The doubling of some of the bands in the fourth derivative may be an indication that δ(C=O) has significantly lower frequency. The frequency of the ν_1 band in 1,4-O_2AQ^{2-} might suggest that it has the same normal mode character as ν_3 in 1,4-$(OH)_2$AQ. Two observations argue against this assignment. First, if the vibrational mode active in 1,4-O_2AQ^{2-} has normal mode character similar to that of the ν_3 vibration in 1,4-$(OH)_2$AQ, the frequency would be greatly altered. The MNDO calculation of the bond order changes in 1,4-$(OH)_2$AQ between the HOMO and LUMO indicated that the active vibration contains a large percentage of C–O stretching character and that this bond is markedly altered upon deprotonation. Second, the transition in the dianion apparently has different characteristics from that of the parent, since the energy of the visible transition shifts in an opposite direction in response to solvent polarity perturbations. MNDO calculations will demonstrate that an electronic excitation from the HOMO to LUMO in 1,4-O_2AQ^{2-} results in the displacement of different internal coordinates from those found for the same transition in 1,4-$(OH)_2$AQ.

Table 3

Wavelengths of the observed bands of 1,4-O_2AQ^{2-} in DMSO and assignments

Wavelength (nm)	Assignment	Frequency above origin (cm^{-1})
626	0-0	0
580	ν_1	+1300
536	$2\nu_1$	+2700

3.2.2. *MNDO calculations*

The π-electron coefficients for the HOMO and LUMO of 1,4-O_2AQ^{2-} calculated using MNDO methods are given in table 4. The geometry used

Table 4

π-electron coefficients for the HOMO and LUMO of 1,4-O_2AQ^{2-} as determined from MNDO calculations

Atom	HOMO	LUMO
O1	0.382	0.154
O9	0.242	−0.155
O4	−0.378	−0.151
O10	−0.239	0.145
C1	−0.198	−0.124
C2	−0.176	−0.166
C3	0.177	0.166
C4	0.199	0.126
C11	0.422	0.063
C10	0.159	−0.109
C12	0.113	−0.429
C5	−0.045	−0.074
C6	−0.088	0.453
C7	0.085	−0.430
C8	0.045	0.031
C13	−0.114	0.457
C9	−0.159	0.112
C14	−0.425	−0.068

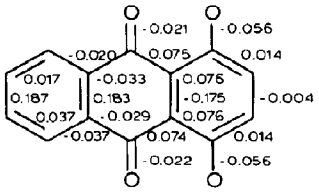

Fig. 6. The π bond order changes for the HOMO to LUMO transition in the dianion of 1,4-dihydroxyanthraquinone as determined from MNDO calculations.

was that of the X-ray crystal structure of 1,4-$(OH)_2$AQ with the protons removed. Although the overall geometry of the dianion may be significantly different, in particular with respect to the C–O and C=O bond distances (and thus more symmetry could be expected in the π-electron coefficients), attempts to determine the minimized geometry using MNDO were unable to achieve self-consistency. Nonetheless, the resulting description of the orbitals fits the experimental observations remarkably well.

The HOMO to LUMO transition of 1,4-O_2AQ^{2-} results in an excitation to an orbital of higher dipole moment with electron density shifted towards the A ring. This is in contrast to the result for 1,4-$(OH)_2$AQ in which the LUMO has a lower dipole moment than the HOMO, but in agreement with the observed shifts in the absorption bands of 1,4-O_2AQ^{2-} in solvents of higher polarity. In addition, both the carbonyl and hydroxy oxygens have decreased electron density in the LUMO. This would explain the blue shift of the absorption band in hydrogen bonding solvents. The transition of the dianion would appear to be charge transfer like, but the electron is moving primarily from the oxygens to the A ring of the molecule.

The π-bond order changes for the HOMO to LUMO transition in 1,4-O_2AQ^{2-} are shown in fig. 6. Although the bond order changes contain some internal coordinate character similar to the primary displacements in 1,4-$(OH)_2$AQ, the dominant vibrational feature is the increase of the C–C bond of the A ring, and C=C bonds of the B ring. A mode with similar internal coordinates is calculated to have a frequency of 1302 cm^{-1} in the ground state of 1,4-$(OH)_2$AQ [51,52]. These results indicate that the similarity in frequency of the excited-state vibrational modes in 1,4-$(OH)_2$AQ and 1,4-O_2AQ^{2-} is fortuitous, and should not be taken as an indication that the visible transitions in these molecules are equivalent. As discussed below, the visible absorption bands of the metal chelates closely mimic the properties of the 1,4-O_2AQ^{2-} spectrum.

3.3. Metal complexes

Upon mixing a metal salt and triethylamine with 1,4-$(OH)_2$AQ in an organic solvent, visible

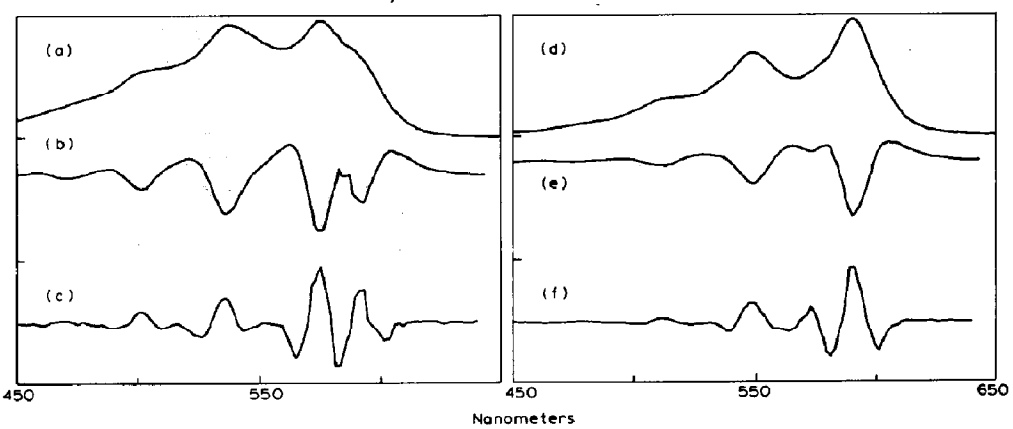

Fig. 7. Absorption spectrum for (a) a 1:1 ratio of 1,4-dihydroxyanthraquinone (1 mM), and $Ni(ClO_4)_2 \cdot 6H_2O$ and triethylamine in ethanol; (b) second derivative of the spectrum in (a); (c) fourth derivative of the spectrum in (a); (d) a 2:1 ratio of 1,4-dihydroxyanthraquinone (1 mM), and $Ni(ClO_4)_2 \cdot 6H_2O$ and triethylamine in ethanol; (e) second derivative of the spectrum in (d); and (f) fourth derivative of the spectrum in (d).

absorption spectra with characteristics similar to those of 1,4-O_2AQ^{2-} are observed. The second and fourth derivatives of these absorption spectra, however, reveal many bands are present which depend on the ratio of the metal and 1,4-$(OH)_2AQ$, the solvent, and the identity of the metal. An example of a typical result is displayed in the spectra of the nickel complexes in ethanol shown in fig. 7. As revealed by the fourth derivative of the spectrum (fig. 7c), two sets of bands are observed in solutions containing a 1 : 1 ratio of Ni(II) and triethylamine to 1,4-$(OH)_2AQ$. (Some of the weak bands observed in fig. 7c are due to unreacted 1,4-$(OH)_2AQ$ in the solution.) The longer wavelength set of bands dominate when a 2 : 1 ratio of Ni(II) and triethylamine to 1,4-$(OH)_2AQ$ is used (fig. 7f). The similarity of the spectrum of the metal-chelated ligand with that of the dianion appears to confirm that the metal binds with removal of the hydroxyl protons and is chelated between the hydroxyl and carbonyl oxygen.

In the following sections, the formation of each of the metal complexes will be discussed individually, and equilibria are elaborated in terms of the observed spectra.

3.3.1. Copper complexes

Much of the previous work on the metal chelates of hydroxyquinones has been with copper complexes. Binuclear Cu(II) chelates of the dianion of 5,8-dihydroxy-1,4-naphthoquinone have been prepared and characterized [4]. These studies indicated a tetrahedral geometry about the central metal atom with an unpaired electron at each Cu(II). A 1,4-$(OH)_2AQ$ polymer formed with Cu(II) in a 1 : 1 stoichiometry has also been studied [8]. The infrared absorption of the C=O stretching frequency in both of these species is approximately equal, indicating similar binding of the metal in the monomer and polymer. Additional reports of copper complexes of the 1,4-$(OH)_2AQ$ system have focused on the anthracycline antibiotics doxorubicin and daunorubicin. Conflicting results have been reported that a complex formed from one metal ion and two drug molecules can be prevalent in aqueous solution at high pH (8.2) [26] or low pH (5.8) [24], and a 1 : 1 stoichiometry

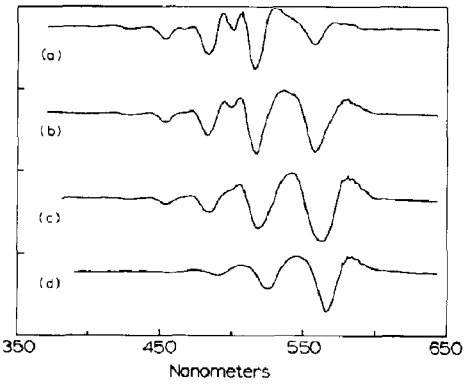

Fig. 8. Second derivative of the absorption spectra of 1,4-dihydroxyanthraquinone with (a) 0.2, (b) 0.6, (c) 1.2 and (d) 2.4 equiv. Cu(II). Cu(II) was supplied as described in the text.

dominates in the opposite pH regime. 1 : 1 polymers appear if the pH is increased above approx. 8.3 [26] or 7.2 [24]. In ethanol sharper absorption bands are observed and both the 1 : 2 and 1 : 1 complexes appear to be formed.

Our studies of the metal complexes are initiated with Cu(II) because of the ease of formation of these species. Upon addition of $Cu(ClO_4)_2 \cdot 6H_2O$ to an ethanolic solution of 1,4-$(OH)_2AQ$, dramatic changes in the absorption spectrum are observed, as shown earlier (fig. 2). A titration of a 1 mM solution of 1,4-$(OH)_2AQ$ with Cu(II) shows gradual changes taking place. The individual absorption bands of the species that are produced in the solution during different points in the titration can be monitored using the second and fourth derivatives of the absorption spectrum. Several representative second derivative spectra from the titration are shown in fig. 8. Upon addition of 0.2 equiv. Cu(II), a small band at 558 nm is observed in the second and fourth derivative, as are several additional smaller bands toward longer wavelength (fig. 8a). The 558 nm band reaches a maximum at 0.6 equiv. Cu(II), and a band at 568 nm is perceived (fig. 8b). Additional Cu(II) causes the 558 nm band to decrease in intensity, while the 568 nm band (and associated vibrational bands) are found to increase rapidly (fig. 8c). No additional changes are observed in the spectrum after slightly greater than approx. 2 equiv. Cu(II) are added, and all of the original bands due to 1,4-$(OH)_2AQ$ have disappeared.

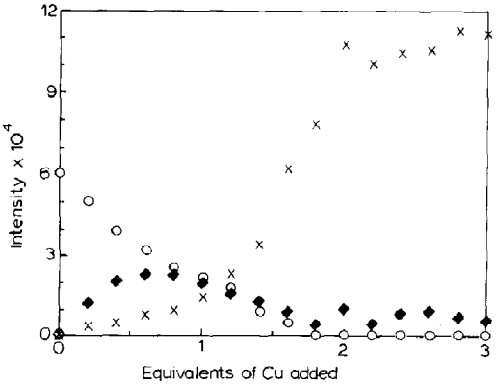

Fig. 9. Fourth derivative intensities (above zero) during the titration of 1,4-dihydroxyanthraquinone with Cu(II): (○) 500 nm band; (◆) 558 nm band; and (×) 568 nm band.

In previous investigations of a titration of daunorubicin in ethanol with Cu(II), it was indicated that there was no isosbestic point in the absorption spectra when greater than 1 equiv. Cu(II) was added. Utilizing the second and fourth derivatives of the absorption spectrum, each of the individual bands can be monitored and the reason for the lack of an isosbestic point discerned. A plot of the fourth derivative intensity vs the equivalents of Cu(II) for each of the bands indicates that there are a minimum of three different species in the solution at any one time. In fig. 9, the fourth derivative intensity of the 1,4-$(OH)_2$AQ bands at 500, 558 and 568 nm are plotted vs equivalents of Cu(II). The 1,4-$(OH)_2$AQ concentration steadily decreases as a function of Cu(II) concentration, and becomes undetectable above 1.8 equiv. The 558 nm band rapidly increases in intensity, maximizing at 0.6 equiv. Cu(II), and falling until 2.0 equiv. are added. Early in the titration the 568 nm band slowly increases in intensity. After 1 equiv. Cu(II) has been added, the band rapidly increases until it plateaus at 2 equiv. Cu(II). Other bands observed in the spectrum appear to follow one of these three patterns during the titration.

Comparison of our observed titration results with previous visible absorption, CD, ^{1}H-NMR and EPR spectroscopy of the copper complexes of doxorubicin and daunorubicin [26] allows assignment of the stoichiometry of the complexes. The saturation of the 568 nm band intensity at slightly greater than 2 equiv. Cu(II) suggests that this complex contains two Cu^{2+} bound to the ligand, forming a 2 : 1 chelate. (In our shorthand notation the number of metal ions will be indicated first.) Similarly, since the 558 nm band intensity maximum occurs approx. at 0.6 equiv. Cu(II), it is likely that the species formed is a 1 : 2 chelate.

The similarity between the vibrational patterns of the metal-chelated ligand and the anionic form of the ligand suggests that the primary character of the excited state involved in this absorption band is localized within the π structure of the ligand (i.e., charge transfer metal-ligand states do not appear to be important in this wavelength region). Since both 1 : 2 and 1 : 1 complexes result in the removal of one proton from the ligand, it would be expected that the 1 : 1 and 1 : 2 complexes have similar wavelengths and extinction coefficients for the observed transitions. This expectation implies that the 558 nm band can be due to either a 1 : 2 or 1 : 1 complex depending on the number of equivalents of Cu(II) added.

Confirmation of these expectations comes from consideration of the observed intensities during the titration. The total concentration of hydroxyanthraquinone chromophores (C_T) must remain constant during the addition of copper. If, initially, only the 1 : 2 and 2 : 1 complexes exist in solution, then

$$C_T = C_{(1,4\text{-}(OH)2AQ)} + 0.5C_{(1:2)} + C_{(2:1)} \quad (1)$$

where C denotes the concentration of the species. Using the titration data of fig. 9, $C_{(1:2)}$ can be calculated from the intensity of the 558 nm band and $C_{(2:1)}$ from the 568 nm band. The data indicate that eq. (1) is valid until greater than 0.6 equiv. Cu(II) have been added. After 0.6 equiv. Cu(II) have been added, the 558 nm band is found to be due to the 1 : 1 species and

$$C_T = C_{(1,4\text{-}(OH)2AQ)} + C_{(1:1)} + C_{(2:1)}. \quad (2)$$

Therefore, at low Cu(II) concentrations the 1 : 2 species dominates; intermediate Cu(II) concentrations yield a mixture of 1 : 1 and 2 : 1 species, while high concentrations of Cu(II) yield exclu-

Table 5

Band positions for the 1:1 (and 1:2) metal complexes of 1,4-(dihydroxy)-9,10-anthraquinone in different solvents as observed from the second and fourth derivatives of the absorption spectrum (– denotes bands that were to weak to detect)

Metal	Wavelength (nm)			
	Ethanol	DMSO	DMF	Pyridine
Zinc	–	568	580	575
	–	530	537	537
	–	494	500	501
Copper	558	560	568	568
	–	–	–	524
	–	–	–	–
Nickel	573	578	585	586
	533	537	545	543
	500	507	511	507
Cobalt	589	600	605	593
	540	550	558	547
	501	–	516	507

sively a 2 : 1 chelate. These titration data represent the first detailed study of the formation of these chelates and is only possible because of the use of the second and fourth derivatives. Assigned bands for each of the metal chelates are tabulated in tables 5 and 6 for the 1 : 1 and 2 : 1 complexes, respectively. Although the wavelengths of the 1 : 1 and 1 : 2 compounds should not necessarily be identical, they could not be distinguished in the spectra.

Table 6

Band positions for the 2 : 1 metal complexes of 1,4-(dihydroxy)-9,10-anthraquinone in different solvents as observed in the second and fourth derivatives of the absorption spectrum (–, band too weak to detect)

Metal	Wavelength (nm)			
	Ethanol	DMSO	DMF	Pyridine
Zinc	–	579	587	591
	–	–	–	–
	–	–	–	–
Copper	568	582	575	580
	525	537	533	534
	483	499	495	500
Nickel	588	599	605	611
	548	555	560	562
	510	512	516	518
Cobalt	605	616	625	620
	–	–	–	571
	–	–	–	530

The reaction of Cu(II) with 1,4-$(OH)_2$AQ can be facilitated with small additions of triethylamine as discussed in section 2. Stoichiometric additions of the base permit the formation of the 2 : 1 complex to dominate in ethanol, but more importantly allow study of additional salts and different solvents. For the copper complexes one observes that the 1 : 1 complex becomes more dominant as one proceeds across the solvent series from DMSO to DMF to pyridine, and it becomes more difficult to form the 2 : 1 complex. In addition, the absorption bands of all the complexes are strongly shifted to longer wavelength along the same solvent series. No effect on the absorption bands is observed if the counterion of the salt is changed. Since this pattern of band shifts is independent of solvent dielectric constant, and the shifts are dramatic compared to those observed for the dianion itself, it appears that the solvent binds the metal at the free coordination sites in each of the complexes. This would explain the strong effect of the solvent on the electronic properties of these systems as discussed in section 4.

3.3.2. Nickel complexes

Similar to the copper complexes, nickel chelates are also readily formed by addition of $Ni(ClO_4) \cdot 6H_2O$ to an ethanolic solution of 1,4-$(OH)_2$AQ. As shown in fig. 7 a 573 nm band dominates the spectrum in ethanol when 1 equiv. Ni(II) and triethylamine are added; however, a 588 nm band dominates when 2 equiv. nickel and triethylamine are added. Associated vibrational structure can be assigned with each of these dominant bands (tables 5 and 6). In contrast to the copper chelates, however, when 2 equiv. Ni(II) are added, the 573 nm band retains intensity even though it results from the 1 : 1 complex. The similarity of the structure of the visible absorption spectra of the copper and nickel complexes with that of the 1,4-O_2AQ^{2-} spectrum again demonstrates that the primary electronic character of the absorption band being analyzed is due to the anionic form of the ligand.

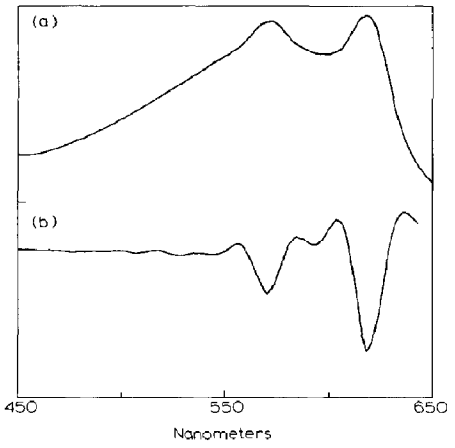

Fig. 10. Absorption spectrum of 1,4-dihydroxyanthraquinone in pyridine (1 mM) with (a) 2 mM $Co(ClO_4)_2 \cdot 6H_2O$ and 2 mM triethylamine; and (b) second derivative of the spectrum in (a).

Comparison of the nickel and copper spectra of the complexes leads to assignment of the shorter wavelength 573 nm band in the nickel complexes to a 1 : 1 species (or a 1 : 2 species at lower Ni(II) concentrations) while the longer wavelength 588 nm band in ethanol is assigned to a 2 : 1 species. The formation of the 2 : 1 Ni(II) complex, however, is not nearly as complete as for the copper chelates. As shown in tables 5 and 6, the spectra

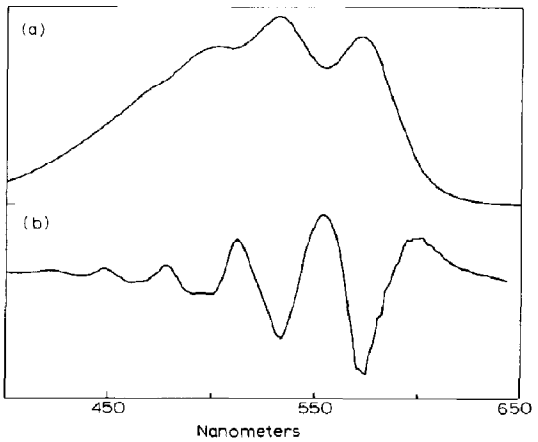

Fig. 11. Absorption spectrum of 1,4-dihydroxyanthraquinone in pyridine (1 mM) with (a) 2 mM $Zn(NO_3)_2 \cdot 6H_2O$ and 2 mM triethylamine; and (b) second derivative of the spectrum in (a).

of the nickel complexes are shifted to longer wavelength with the solvent series ethanol, DMSO, DMF and pyridine. Unlike the copper complexes, however, pyridine does not inhibit the formation of the 2 : 1 complex, and the 2 : 1 chelate dominates when two equivalents of nickel and triethylamine are added to a solution of 1,4-$(OH)_2$AQ in pyridine.

3.3.3. Cobalt and zinc complexes

Neither the cobalt nor zinc chelates of 1,4-$(OH)_2$AQ are formed easily in ethanol, DMSO or DMF. The second derivative of the absorption spectrum measured after the addition of 1 equiv. cobalt or zinc and triethylamine to a solution of 1,4-$(OH)_2$AQ indicates that much of the original 1,4-$(OH)_2$AQ has not reacted. Zinc barely complexes in ethanol even if 2 equiv. of metal and base are added. Formation of the chelates is most complete for both of these metals in pyridine, contrasting with the results obtained for both copper and nickel.

The spectrum of cobalt and zinc complexes in pyridine with 2 equiv. metal and triethylamine added are shown in figs. 10 and 11, respectively. The similarity in structure of these spectra and their derivatives with those of the copper and nickel chelates is again an indication that the absorption band is primarily due to anionic forms of the ligand. The bands are shifted to longer wavelength in solvents similar to copper and nickel. The exception is the bands of the cobalt complexes in pyridine which are at shorter wavelengths than in DMF. The absorption bands of the zinc complexes are at the shortest wavelengths compared to the other metal chelates while those of the cobalt complexes are at the longest wavelengths.

4. Conclusions

Detailed studies of the visible absorption spectrum of 1,4-$(OH)_2$AQ and its metal chelates have been carried out. Utilization of the second and fourth derivatives of the absorption band permits characterization of all the species formed in several different organic solvents. For the parent com-

pound, the results indicate that the lowest excited state has a reduced dipole moment compared to the ground state, in agreement with previous work [31]. In contrast, the character of the excited state changes upon deprotonation and interaction with transition metals, and a vibration of different composition becomes active.

The visible absorption spectra show that the transition metals will react in 1:2, 1:1 and 2:1 ratios with 1,4-$(OH)_2$AQ depending on the metal, its relative concentration, and the solvent. The reactions can be aided by the stoichiometric addition of triethylamine, a weak base which binds released protons from 1,4-$(OH)_2$AQ during the chelation process. The visible absorption spectra of the metal chelate resemble that of the dianion of the parent complex with bathochromic shifts determined by the identity of the metal and solvent.

Understanding the electronic characteristics of the observed visible absorption spectrum of these complexes can aid in using the absorption spectra to establish the mechanism of action of the anthracycline antibiotics, doxorubicin and daunorubicin. In particular, the role of the metal chelates in the antitumor activity of these drugs can be probed. Resonance Raman studies are currently underway which will extend many of the vibrational and electronic characteristics described in this paper, and allow study of the chelates in the presence of DNA.

Acknowledgments

Acknowledgment is made to the Donors of the Petroleum Research Fund, administered by the American Chemical Society for partial support of this research. This research was also supported in part by a grant from Research Corporation and the SUNY Research Foundation.

References

1 R.H. Thomson, Naturally occurring quinones (Academic Press, New York, 1971).
2 P.K. Dutta and J.A. Hutt, J. Raman. Spectrosc. 18 (1987) 339.
3 M.N. Bakola-Christianopoulou, Polyhedron 3 (1984) 729.
4 C.A. Tsipis, E.G. Bakalbassis, V.P. Papageorgiou and M.N. Bakola-Christianopoulou, Can. J. Chem. 60 (1982) 2477.
5 R. Kiraly and R.B. Martin, Inorg. Chim. Acta 67 (1982) 13.
6 B. Bogdanovic and M. Yus, Angew. Chem. Int. Ed. Engl. 91 (1979) 681.
7 P.H. Merrell, Inorg. Chim. Acta 32 (1979) 99.
8 D.A. Lusardi, Ph.D. thesis, University of Notre Dame, Notre Dame, Indiana (1978).
9 D.L. Van Duuren, A. Segal, S.S. Tseng, G.M. Rusch, G. Loewengart, U. Mate, D. Roth, A. Smith and S. Melchionne, J. Med. Chem. 21 (1978) 26.
10 S.B. Padhye, C.R. Joshi and B.A. Kulkarni, J. Inorg. Nucl. Chem. 39 (1977) 1289.
11 H.D. Coble and H.F. Holtzclaw, Jr, J. Inorg. Nucl. Chem. 36 (1974) 1049.
12 A. Dufrense, C.G. de Lima, J. Knudsen and J.E. Moreira, J. Inorg. Nucl. Chem. 35 (1973) 789.
13 B.E. Zaitsev, N.P. Vasileva and B.N. Ivanov-Emin, Russ. J. Inorg. Chem. 16 (1971) 502.
14 R.S. Bottei and C.P. McEachern, J. Inorg. Nucl. Chem. 32 (1970) 2653.
15 R.S. Bottei and D.J. Quane, Inorg. Nucl. Chem. 26 (1964) 1919.
16 R.S. Bottei and P.L. Gerace, J. Inorg. Nucl. Chem. 23 (1961) 245.
17 F. Arcamone, Doxorubicin: Anticancer antibiotics (Academic Press, New York, 1981).
18 W.A. Remers, The chemistry of antitumor antibiotics (Wiley, New York, 1979) p. 63.
19 J.C. Wang, Biochim. Biophys. Acta 909 (1987) 1.
20 J.W. Lown, S.-K. Sim and H.-H. Chem, Can. J. Biochem. 56 (1978) 1042.
21 M.M.L. Fiallo and A. Garnier-Suillerot, Biochemistry 25 (1986) 924.
22 H. Beraldo, A. Garnier-Suillerot, L. Tosi and F. Lavelle, Biochemistry 24 (1985) 284.
23 P.K. Dutta and J.A. Hutt, Biochemistry 25 (1986) 691.
24 H. Beraldo, A. Garnier-Suillerot and L. Tosi, Inorg. Chem. 22 (1983) 4117.
25 C.E. Myers, L. Gianni, C.B. Simone, R. Klecker and R. Greene, Biochemistry 21 (1982) 1707.
26 F.T. Greenaway and J.C. Dabrowiak, J. Inorg. Biochem. 16 (1982) 91.
27 M. Spinelli and J.C. Dabrowiak, Biochemistry 21 (1982) 5862.
28 D.R. Phillips and G.A. Carlyle, Biochem. Pharmacol. 30 (1981) 2021.
29 P. Mikelens and W. Levinson, Bioinorg. Chem. 9 (1978) 441.
30 E. Calendi, A. DiMarco, M. Reggiani, B. Scarpinato and L. Valentini, Biochim. Biophys. Acta 103 (1965) 25.
31 L.W. Johnson, M.A. Savory, C. Pope, M. Foresti and J.R. Lombardi, J. Chem. Phys. 86 (1987) 3048.
32 G. Smulevich and P.J. Foggi, Chem. Phys. 87 (1987) 5657.

33 G. Smulevich, P. Foggi, A. Feis and M.P. Marzocchi, J. Chem. Phys. 87 (1987) 5664.
34 G. Smulevich and M.P. Marzocchi, Chem. Phys. 105 (1986) 159.
35 G. Smulevich, J. Chem. Phys. 82 (1985) 14.
36 M.H. van Benthem and G.D. Gillispie, J. Phys. Chem. 88 (1984) 2954.
37 G. Smulevich, L. Angeloni, S. Giovannardi and M.P. Marzocchi, Chem. Phys. 65 (1982) 313.
38 R.N. Capps and M. Vala, Photochem. Photobiol. 33 (1981) 673.
39 W.F. Maddams, Makromol. Chem., Macromol. Symp. 5 (1986) 35.
40 W.F. Maddams and W.L. Mead, Spectrochim. Acta 38A (1982) 437.
41 W.F. Maddams, Appl. Spectrosc. 34 (1980) 245.
42 W.L. Butler and D.W. Hopkins, Photochem. Photobiol. 12 (1970) 439.
43 W.L. Butler and D.W. Hopkins, Photochem. Photobiol. 12 (1970) 451.
44 T.C. O'Haver and G.L. Green, Anal. Chem. 48 (1976) 312.
45 S.B. Hastie and R.P. Rava, J. Am. Chem. Soc. 111 (1989) 6993.
46 M.J.S. Dewar and W.J. Thiel, J. Am. Chem. Soc. 99 (1977) 4899.
47 S.R. Martin, Biopolymers 19 (1980) 713.
48 F. Drissler, F. Graf and D.J. Haarer, Chem. Phys. 72 (1980) 4996.
49 F. Graf, H.K. Hong, A. Nazzal and D. Haarer, Chem. Phys. Lett. 59 (1978) 217.
50 G.D. Nigam and B.Z. Deppisch, Kristallogr. 151 (1980) 185.
51 A.N. Anoshin, E.A. Gastolivich, K.A. Mishenina and D.N. Shigorin, Russ. J. Phys. Chem. 57 (1983) 861.
52 A.N. Anoshin, E.A. Gastolivich, M.V. Gorelik, T.S. Kopteva and D.N. Shigorin, Russ. J. Phys. Chem. 56 (1982) 1011.
53 I.J. McLennan and R.E. Lenkinski, J. Am. Chem. Soc. 106 (1984) 6905.